

Quality Assessment Report

GEOV2-AVHRR: Leaf Area Index (LAI), Fraction of Absorbed Photosynthetically Active Radiation (FAPAR) and Fraction of green Vegetation Cover (FCOVER) from LTDR AVHRR

THEIA-RP-44-0281-CREAF

Issue I1.10

Submission date: 24.09.2020

Start of the project: 18.09.2014

Organization name of lead contractor for this deliverable: CREAM

Author: Alexandre Verger (CREAF)

Document Release Sheet

Book captain:	Aleixandre Verger		Sign	Date 24.09.2020
Approval:	Philippe Pacholczyk		Sign	Date 24.09.2020
Endorsement:	Marc Leroy		Sign	Date
Distribution:				

Change Record

Issue/Rev	Date	Page(s)	Description of Change	Release
	2.12.2015	All	First Issue	I1.00
I1.00	24.09.2020	All	Updated validation	I1.10

TABLE OF CONTENTS

1	<i>Background of the document</i>	9
1.1	Executive Summary	9
1.2	Scope and Objectives.....	9
1.3	Content of the document.....	9
1.4	Related documents	10
1.4.1	Applicable documents	10
2	<i>Quality assessment of GEOV2-AVHRR products</i>	11
2.1	Temporal profiles over a sample of sites	11
2.2	Comparison with GEOV2-CGLS, GIMMS3g and GLASS	19
2.3	Spatio-temporal continuity	29
2.4	Temporal smoothness	31
2.5	Consistency between LAI, FAPAR and FCOVER products	32
2.6	Comparison with ground data.....	34
3	<i>Conclusion</i>	36
4	<i>References</i>	37

LIST OF FIGURES

Figure 1: Temporal profile of GEOV2-AVHRR, GEOV2-CGLS, GIMMS3g and GLASS products over two typical evergreen broadleaf forest site for the period 1981-2019.	14
Figure 2: Idem Figure 1 for two typical Deciduous Broadleaf Forest sites.	15
Figure 3: Idem Figure 1 for two typical Needleleaf Forest sites.	16
Figure 4: Idem Figure 1 for two typical Crop sites.	17
Figure 5: Idem Figure 1 for two typical Shrub-Savana-Bare sites.	18
Figure 6: Mean GEOV2-AVHRR LAI values (top) and mean LAI differences between GEOV2-AVHRR and GEOV2-CGLS, GIMMS3g, and GLASS products for the common period for winter and summer solstice dates. Red (blue) tones in the maps of differences indicate positive (negative) differences, i.e. higher (lower) GEOV2-AVHRR values. The areas in grey correspond to pixels with no data.	21
Figure 7: Idem Figure 6 but for FAPAR.	22
Figure 8: Idem Figure 6 but for FCOVER.	23
Figure 9: Comparison between GEOV2-AVHRR and (a) GEOV2-CGLS, (b) GIMMS3g, (c) GLASS LAI products over the BELMANIP2 sites for the 1999-2011 period.	24
Figure 10: Comparison between GEOV2-AVHRR and (a) GEOV2-CGLS, (b) GIMMS3g, (c) GLASS FAPAR products over the BELMANIP2 sites for the 1999-2011 period	24
Figure 11: Comparison between GEOV2-AVHRR and (a) GEOV2-CGLS, (b) GLASS FCOVER products over the BELMANIP2 sites for the 2000-2016 period.	24
Figure 12: Distribution of GEOV2-AVHRR, GEOV2-CGLS, GIMMS3g and GLASS LAI products per CCI-LC biome type as sampled by the 445 BELMANIP2 sites over the 1999-2011 period.	25
Figure 13: Distribution of GEOV2-AVHRR, GEOV2-CGLS, GIMMS3g and GLASS FAPAR products per CCI-LC biome type as sampled by the 445 BELMANIP2 sites over the 1999-2011 period.	26
Figure 14: Distribution of GEOV2-AVHRR, GEOV2-CGLS and GLASS FCOVER products per CCI-LC biome type as sampled by the 445 BELMANIP2 sites over the 1999-2018 period.	27
Figure 15: Evaluation of the differences between GEOV2-AVHRR and GEOV2-CGLS LAI products over the BELMANIP2.1 sites for the years 1999-2019 as a function of (a) the number of valid AVHRR observations in the compositing period (NOBS) and (b) the GEOV2-AVHRR product uncertainty (i.e., RMSE between the GEOV2-AVHRR product and the daily AVHRR observations in the compositing period). The gray levels correspond to 75% (dark gray), 90% (medium gray) and 95% (light gray) of the population, and the dots to 5% percentile of the residual outliers. The bold back solid line corresponds to the median value of the differences.	

The blue dashed line shows the distribution of values of the variable in the abscissa which frequencies are indicated in the vertical axis on the right. 28

Figure 16: Idem Figure 15 but for FAPAR 28

Figure 17: Idem Figure 15 but for FCOVER 28

Figure 18: (a) Map of the fraction of filled data for which the climatology or the linear interpolation is used for processing GEOV2-AVHRR products. (b) Map of the fraction of gaps for GIMMS3g products. The areas in grey correspond to unprocessed pixels (missing data). Evaluation for the 1981-2011 period..... 30

Figure 19: Average fraction of valid GEOV2-AVHRR and GIMMS3g products per biome. The biome classes are derived from the CCI landcover map (http://maps.elie.ucl.ac.be/CCI/viewer/download/ESACCI-LC-Ph2-PUGv2_2.0.pdf): Shrubs/Savana/Bare soil (SSB), Crops and Grassland (CG), Deciduous Broadleaf Forests (DBF), Needleleaf Forest (NF), and Evergreen Broadleaf Forest (EBF). For GEOV2/AVHRR, high quality products (grey) and products where the climatology was used to fill gaps (less than 12 valid daily estimates exist in the compositing period) (black) are distinguished. Evaluation over the BELMANIP2 sites for the 1981-2011 period. 31

Figure 20: Histogram of the δ LAI absolute difference representing temporal smoothness for GEOV2-AVHRR, GEOV2-CGLS, GIMMS3g and GLASS LAI products. Evaluation over the BELMANIP2 sites for the 1999-2011 period..... 32

Figure 21: Relationship between LAI and FAPAR for GEOV2-CGLS, GEOV2-AVHRR, GIMMS3g and GLASS products as evaluated over the 445 BELMANIP2.1 sites during the 1999-2011 period. The color indicates the density of points from yellow (highest) to blue (lowest density). 33

Figure 22: Relationship between FAPAR and FCOVER for GEOV2-CGLS, GEOV2-AVHRR and GLASS products as evaluated over the 445 BELMANIP2.1 sites during the 2000-2011 period. The color indicates the density of points from yellow (highest) to blue (lowest density). 33

Figure 23: Comparison of GEOV2-AVHRR with ground measurements for (a) LAI, (b) FAPAR and (c) FCOVER in the 1999-2017 period. The different symbols correspond to the five biome classes as derived from the CCI landcover map (http://maps.elie.ucl.ac.be/CCI/viewer/download/ESACCI-LC-Ph2-PUGv2_2.0.pdf). The dotted line corresponds to the 1:1 line. The solid lines represent the GCOS accuracy criteria: max(20%, 0.5) for LAI, max(10%, 0.05) for FAPAR (and FCOVER) (GCOS 2011). The statistics of the comparison are provided in Table 1. 34

LIST OF TABLES

Table 1: Statistics of the comparison of GEOV2-AVHRR, GEOV2-CGLS, GIMMS3g and GLASS with ground measurements for LAI, FAPAR and FCOVER variables over the DIRECT2 sites for the common samples in the 1999-2017 period: number of sites, number of samples (sites x dates), percentage of samples which meet GCOS requirements in terms of accuracy (max(20%, 0.5) for LAI, max(10%, 0.05) for FAPAR (and FCOVER) (GCOS 2011)), root mean square error (RMSE), correlation coefficient (R), slope and offset of the least squares linear regression. (*) Statistics of the validation of GEOV2-AVHRR over all available samples in the 1999-2017 period..... 35

LIST OF ACRONYMS

ATBD	Algorithm theoretical based Document
AVHRR	Advanced Very High Resolution Radiometer
BELMANIP	BEenchmark Land Multisite ANalysis and Intercomparison of Products
BRDF	Bidirectional Reflectance Distribution Function
BS	Bare Soil
CACAO	Consistent Adjustment of Climatology to Actual Observations
CEOS	Committee for Earth Observation Satellite
CGLS	Copernicus Global Land Service
CNES	Centre National d'Études Spatiales (French Space Agency)
CREAF	Centre for Ecological Research and Forestry Applications
CYCLOPES	Carbon cYcle and Change in Land Observational Products from an Ensemble of Satellites
EBF	Evergreen Broadleaf Forest
FAPAR	Fraction of Absorbed Photosynthetically Active Radiation
FCOVER	Fraction of vegetation cover
GCOS	Global Climate Observation System
GEOCLIM	Climatology of Version 1 LAI, FAPAR, FCover VGT products
GEOV1	GEOLAND2 Version 1 product
GEOV2	GEOLAND2 Version 2 product
GIMMS	Global Inventory and Monitoring and Modeling Study
GLASS	Global LAnd Surface Satellite
GTOS	Global Terrestrial Observation System
INRAE	Institut national de recherche pour l'agriculture, l'alimentation et l'environnement (National Research Institute for Agriculture, Food and Environment, France)
LAI	Leaf Area Index
LPV	Land Product Validation group of CEOS
LTDR	Long Time Data Record
MODIS	Moderate Imaging Spectrometer
NDVI	Normalized Difference Vegetation Index
NIR	Near Infrared
NTOC-r	Directionally Normalized Top Of the Canopy reflectances
QC	Quality control indicator
QF	Quality flag
RMSE	Root Mean Square Error
SPOT	Satellite Pour l'Observation de la Terre
SWIR	Short Wave Infrared
SZA	Sun Zenith Angle
TOC	Top of Canopy
TSGF	Temporal Smoothing Gap Filling
VGT	VEGETATION instruhment onboard SPOT satellite

1 BACKGROUND OF THE DOCUMENT

1.1 EXECUTIVE SUMMARY

GEOV2-AVHRR products have been generated by CNES based on the algorithm theoretical baseline description (ATBD) developed by CREAM and INRAE [THEIA-SP-44-0207-CREAM]. GEOV2-AVHRR provides a series of biophysical variables (LAI, FAPAR and FCOVER) on the status and evolution of land surface at the global scale over the 1981-2019 period at 0.05° spatial resolution every ten days. The products are derived from AVHRR LTDR (Long Term Data Record) version 4 reflectance data.

Quality Assessment constitutes the only means of guaranteeing the compliance of generated products with user requirements. It concerns new products which must pass an exhaustive scientific evaluation before to be implemented operationally. The procedure follows, as much as possible, the guidelines, protocols and metrics defined by the Land Product Validation (LPV) group of the Committee on Earth Observation Satellite (CEOS) for the validation of satellite-derived land products.

This document presents a Quality Assessment of GEOV2-AVHRR LAI, FAPAR and FCOVER products during the 1981-2019 period. The analysis is mainly focused on the inter-comparison of GEOV2-AVHRR with similar existing and validated datasets. In particular, GEOV2-AVHRR is compared with the GEOV2-CGLS products derived from VEGETATION and PROBA-V data (Verger et al. 2016). GEOV2-AVHRR and GEOV2-CGLS are based on the ‘same’ retrieval algorithm with minor adaptations to the particularities of the two datasets (Verger et al. 2016). We also compared GEOV2-AVHRR with other products derived from AVHRR time series: i.e., GIMMS3g (Zhu et al. 2013) and GLASS (Jia et al. 2019; Liang et al. 2013) products. Finally, we performed a direct comparison of GEOV2-AVHRR estimates with ground data over a limited number of samples available over the DIRECT2 sites.

1.2 SCOPE AND OBJECTIVES

The scope of this document is to present a quality assessment of GEOV2-AVHRR LAI, FAPAR and FCOVER products over the 1981-2019 period.

GEOV2-AVHRR LAI, FAPAR and FCOVER products are evaluated and compared with existing GEOV2-CGLS, GIMMS3g and GLASS products in terms of consistency, continuity and accuracy.

1.3 CONTENT OF THE DOCUMENT

This document is structured as follows:

Chapter 2. Quality assessment of GEOV2-AVHRR prototyped estimates:

- Temporal profiles over a sample of sites
- Comparison with GEOV2-CGLS, GIMMS3g and GLASS products
- Spatio-temporal continuity

- Temporal smoothness
- Internal consistency between LAI, FAPAR and FCOVER variables
- Accuracy assessment based on the comparison with ground data over the DIRECT2 sites

Chapter 3. Conclusions

1.4 RELATED DOCUMENTS

1.4.1 Applicable documents

Document ID	Descriptor
CNES contract N°140570/00	CNES contracts scientific support of CREAM for the development and validation of the GEOV2-AVHRR products
THEIA-CT-44-0163-CNES	Scientific support requested
THEIA-SP-44-0207-CREAM	Algorithm theoretical baseline description (ATBD) of GEOV2-AVHRR

2 QUALITY ASSESSMENT OF GEOV2-AVHRR PRODUCTS

2.1 TEMPORAL PROFILES OVER A SAMPLE OF SITES

The analysis is organized per large biome type based on the CCI-LC (v1.6.1, epoch 2010 from 2008 to 2012) (<https://www.esa-landcover-cci.org>) land cover map, selecting few sites showing typical temporal profiles. For the evergreen broad leaf forest (Figure 1), the effect of residual clouds is very pronounced, creating strongly negatively biased estimates and noisy temporal profiles in GIMMS3g products. These artefacts are efficiently filtered in the other products which show very flat temporal profiles with a high level of LAI, FAPAR and FCOVER as expected. GEOV2-AVHRR highly agrees with GIMMS3g and GLASS for the maximum LAI values while GEOV2-CGLS systematically shows higher LAI values. Higher agreement between the different products is observed for FAPAR and FCOVER.

For deciduous broadleaf forest (Figure 2), GIMMS3g is also negatively biased and shows some instabilities for the period of the maximum growing season due to cloud contamination (e.g. site #75). In these problematic situations GEOV2-AVHRR, GEOV2-CGLS and GLASS seem to be more robust to the noise in the data and they show more temporally consistent and smooth time evolutions. For very high latitudes (site #262 in Figure 2, and sites #107 and #271 in Figure 3), the highest discrepancies are observed in winter time: GEOV2-AVHRR and GEOV2-CGLS LAI and FAPAR values are higher than GIMMS3g and GLASS ones; and GLASS FCOVER shows systematically higher values than GEOV2-AVHRR and GEOV2-CGLS FCOVER. GIMMS3g products shows some temporal discontinuities in winter time when very few observations are available because of the low illumination conditions and snow cover. Conversely, GEOV2-AVHRR, GEOV2-CGLS and GLASS products are continuous with no interruption during the winter period. In these conditions, LAI, FAPAR and FCOVER GEOV2-AVHRR and GEOV2-CGLS are gap filled and mostly driven by the GEOCLIM climatology (Verger et al. 2015). GLASS shows higher interannual variability with unexpected very high LAI and FAPAR winter values for some years probably due to directional effects for very high sun zenith angles. GLASS LAI and FAPAR show some temporal inconsistencies and do not reproduce the actual annual seasonality for years 1985-1987, 1993 and 2000 over site #262. In these conditions, GLASS FCOVER appears more robust than GLASS LAI/FAPAR and shows higher intra-annual and interannual temporal consistency. The internal consistency of GLASS products is not met: FCOVER values in winter time are systematically higher than GLASS FAPAR which is not expected (see section 2.5).

The different products show a general good agreement for the cropland site #189 with the exception that GIMMS3g reaches slightly higher values in the base level (Figure 4, top). Higher differences between products are observed for the double-cycle site #337 (Figure 4, bottom). GEOV2-AVHRR, GEOV2-CGLS and GIMMS3g show a good agreement in terms of seasonality and they correctly reproduce the two growing cycles of this cropland area. On the contrary, the GLASS LAI and FAPAR products show temporal inconsistencies and significant limitations to correctly reproduce the double seasonality of site #337 (Figure 4, bottom). Again, GLASS FCOVER improves temporal consistency as compared to GLASS LAI/FAPAR.

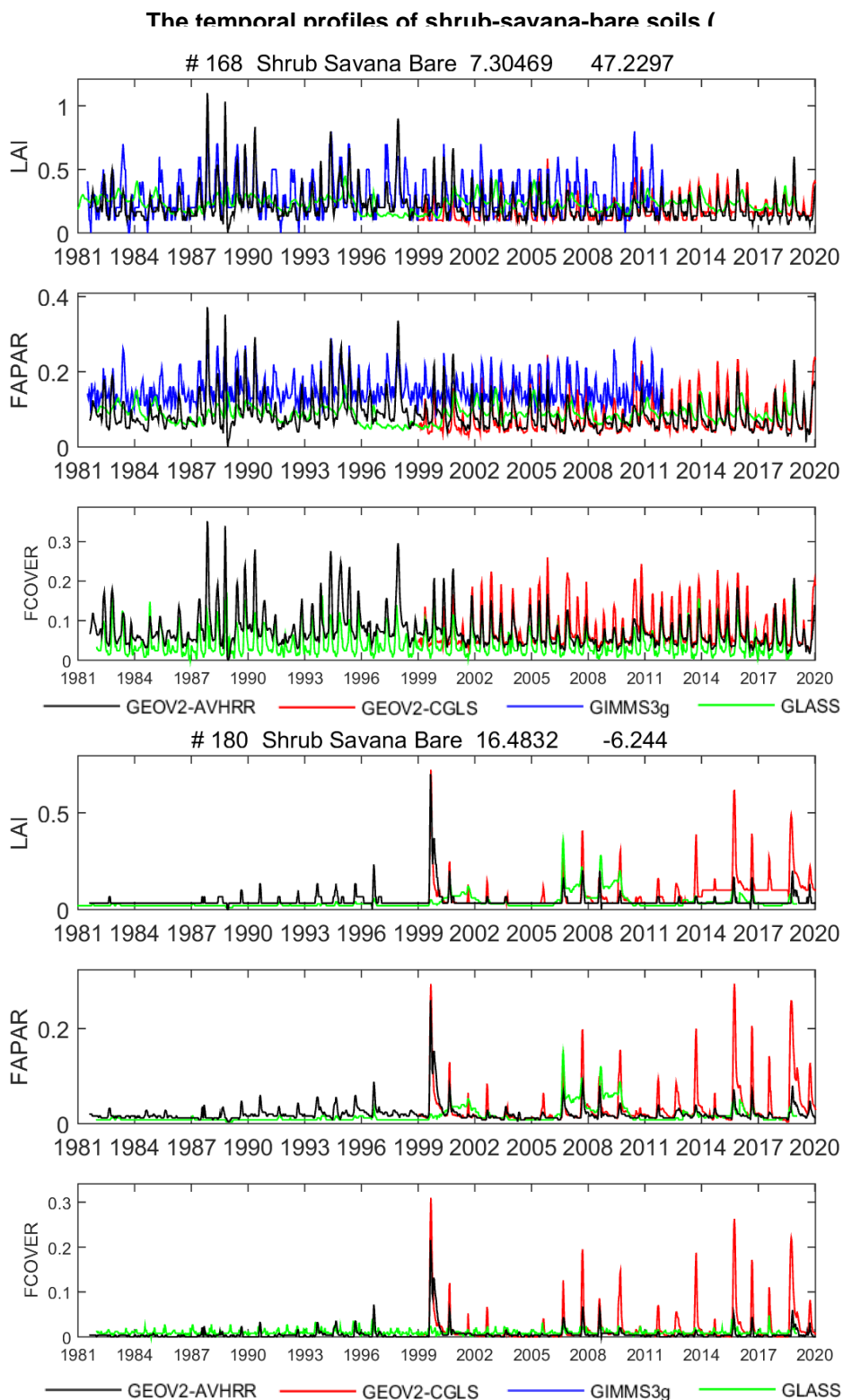


Figure 5) are also very well captured by GEOV2-AVHRR with a very good agreement with GEOV2-CGLS in terms of the magnitude of products and temporal seasonality. GIMMS3g systematically

provides higher FAPAR values (e.g. site #168). GLASS show some limitations to reproduce short annual seasons and rapid temporal changes as illustrated in site #168 and #180. For bare soil areas (e.g. site #180) the GIMMS3g LAI and FAPAR products are not available.

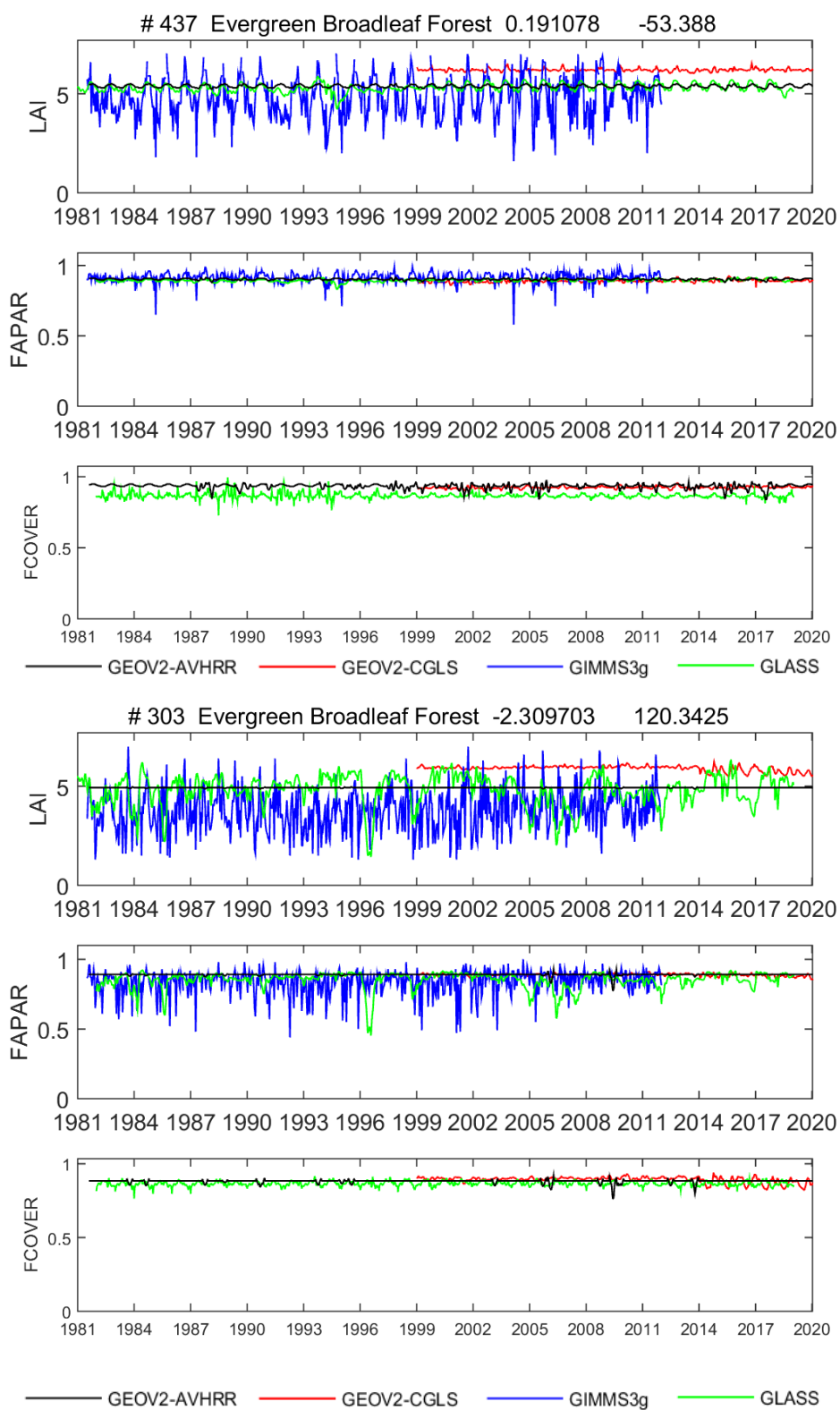


Figure 1: Temporal profile of GEOV2-AVHRR, GEOV2-CGLS, GIMMS3g and GLASS products over two typical evergreen broadleaf forest site for the period 1981-2019.

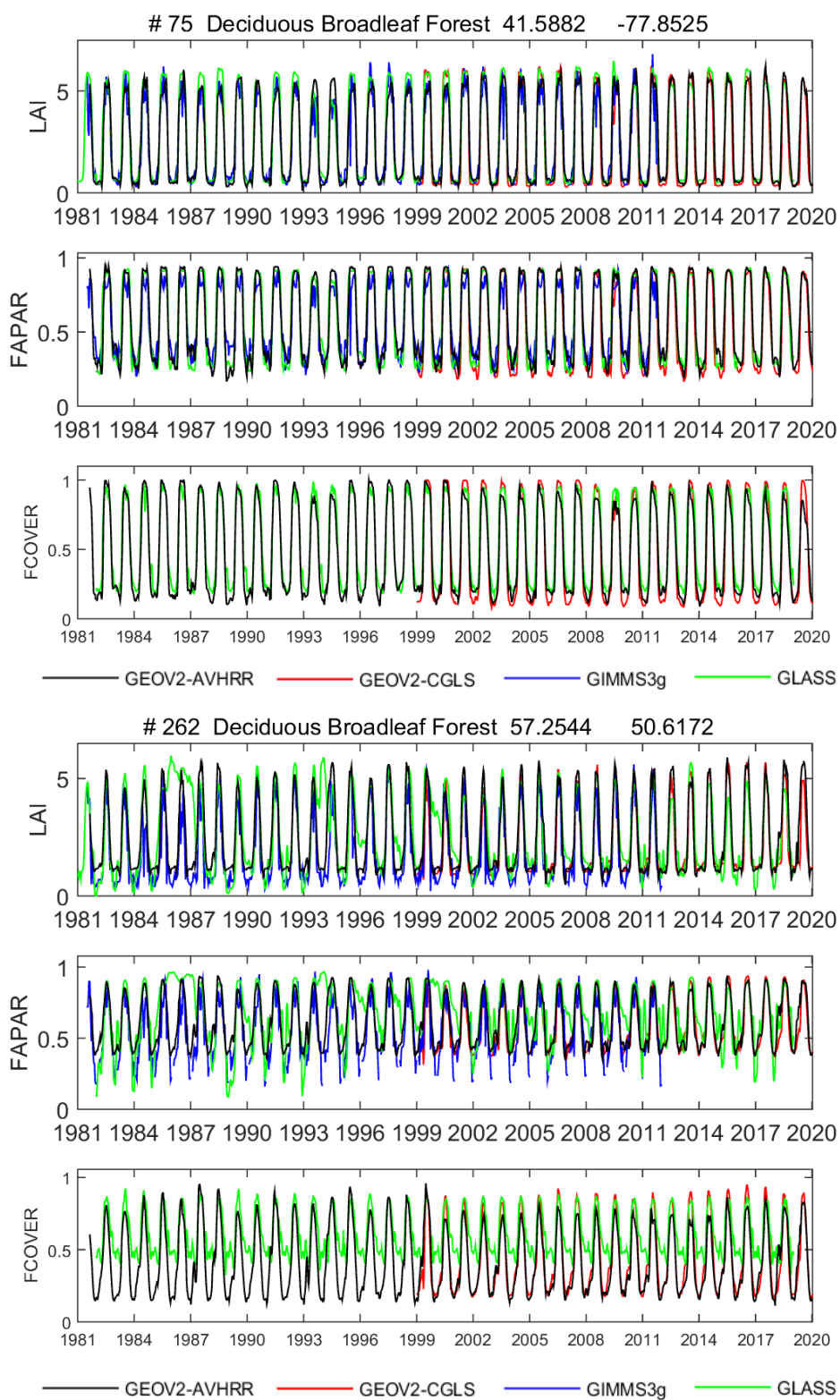


Figure 2: Idem Figure 1 for two typical Deciduous Broadleaf Forest sites.

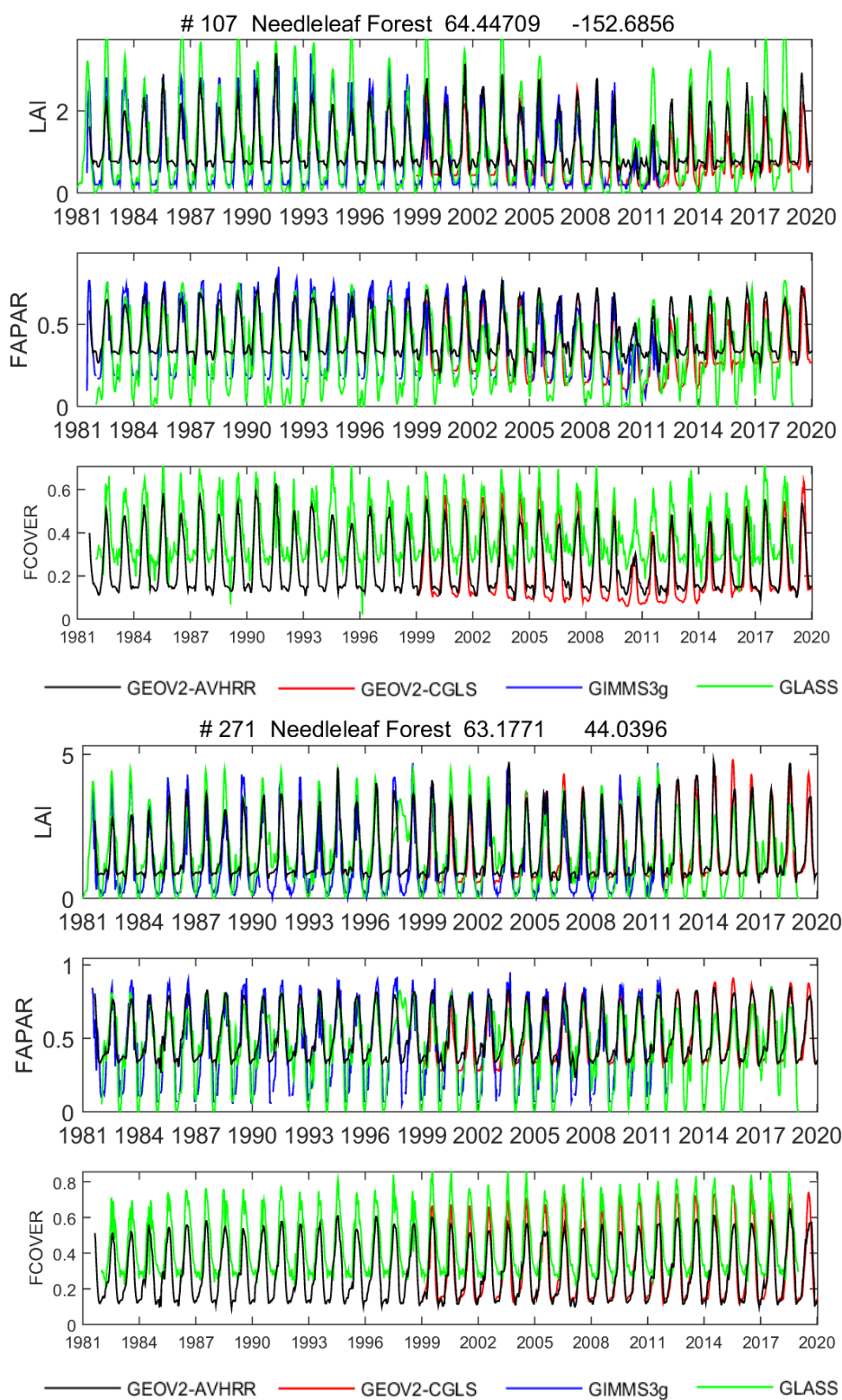


Figure 3: Idem Figure 1 for two typical Needleleaf Forest sites.

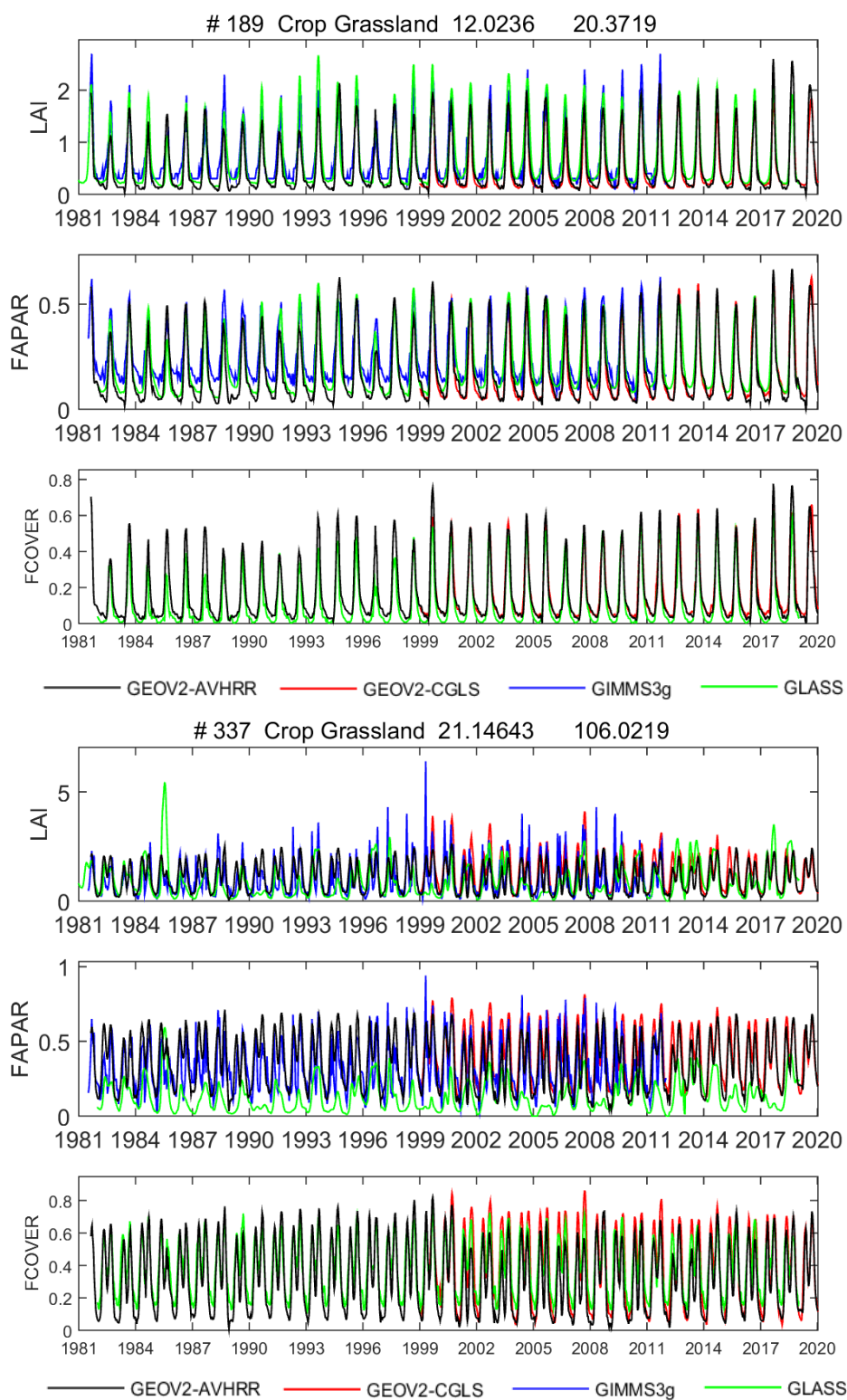


Figure 4: Idem Figure 1 for two typical Crop sites.

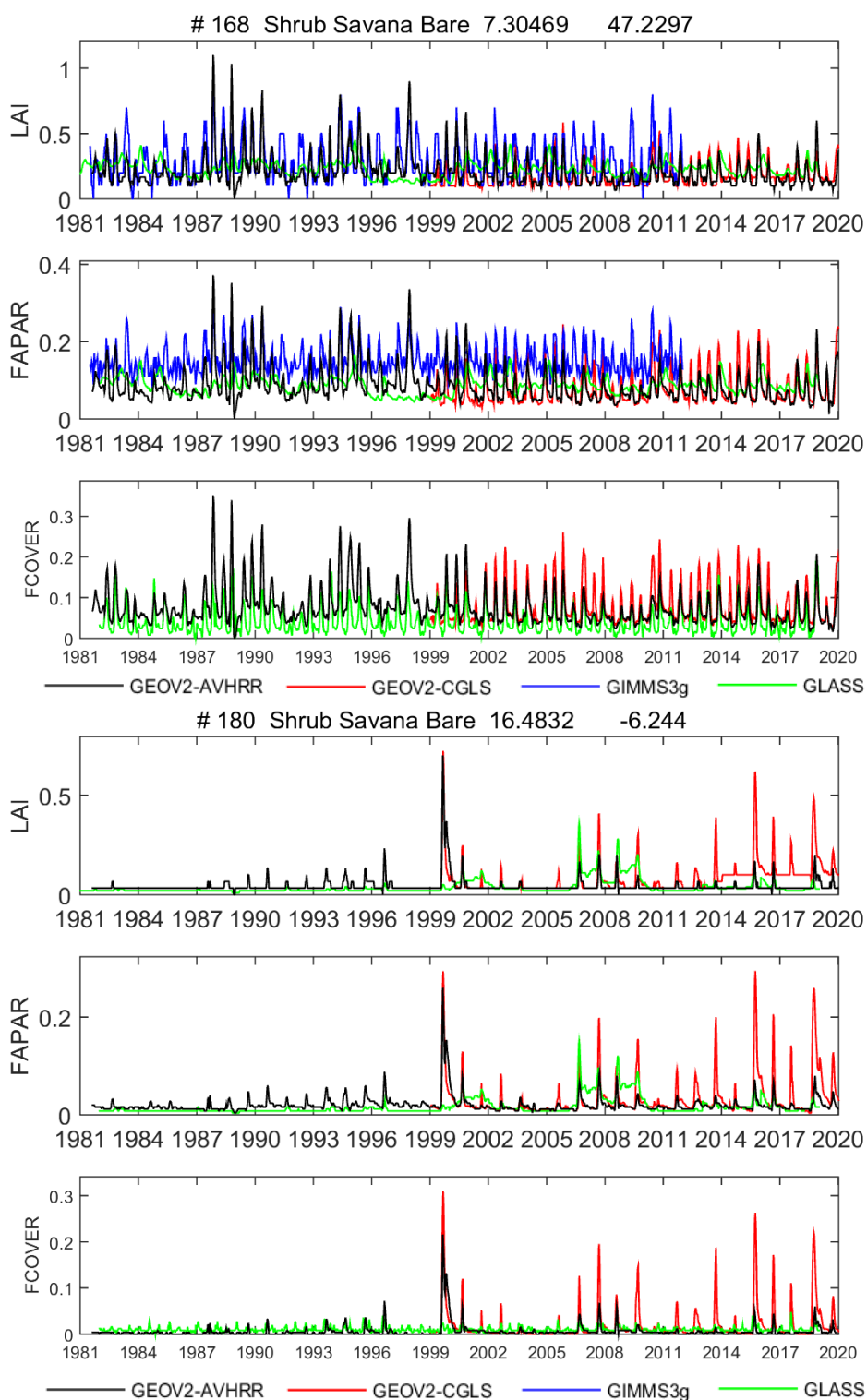


Figure 5: Idem Figure 1 for two typical Shrub-Savana-Bare sites.

2.2 COMPARISON WITH GEOV2-CGLS, GIMMS3g AND GLASS

The comparison of GEOV2-AVHRR with GEOV2-CGLS (1999-2019), GIMMS3g (1981-2011) and GLASS (1981-2018) LAI products shows 94% of land pixels meet GCOS requirements of ± 0.5 LAI differences (Figure 6). The highest differences between LAI products are observed over Evergreen Broadleaf Forests (EBF) at latitudes near the Equator: GEOV2-AVHRR shows systematic lower LAI values than GEOV2-CGLS (blue tones in Figure 6) but higher values than GIMMS3g (red tones in Figure 6) and a good agreement with GLASS (green tones in Figure 6), and over northern high latitudes in winter time: GEOV2-AVHRR shows higher LAI values than GIMMS3g and GLASS (red tones in Figure 6) although highly agrees with GEOV2-CGLS. The scatterplot of the comparison between GEOV2-AVHRR and GEOV2-CGLS LAI products shows a very good agreement (RMSE of 0.53, correlation coefficient of 0.97, slope of the linear regression close to the unity with no offset) (Figure 9a). Similar good agreement is found between GEOV2-AVHRR as compared with GIMMS3g (Figure 9b) and GLASS (Figure 9c) products, although higher scattering is observed. The distributions of LAI values per biomes (Figure 12) are very consistent between GEOV2-AVHRR, GEOV2-CGLS, GIMMS3g and GLASS with higher differences for EBFs due, in part, to the higher uncertainties in the data but also to intrinsic limitations of retrieval algorithms, saturation of the signal as well as differences in the training process. GEOV2-AVHRR and GLASS show very similar distributions for EBFs and agree with GIMMS for the location of the peak: maximum frequencies at LAI=5. GEOV2-CGLS shows maximum frequencies at LAI=6. GIMMS3g shows a broad distribution of LAI values for EBFs which is associated to the noise and instabilities observed in the temporal profiles (Figure 1). The other products exhibit sharp distributions mainly because of the more efficient filtering of cloud contamination and the algorithm assumptions forcing a very limited seasonality for EBFs. For needleleaf forest, GLASS shows slightly lower frequencies for LAI<2 and an unexpected bimodal distribution (Figure 12).

For FAPAR, the comparison between GEOV2-AVHRR and GEOV2-CGLS products shows 85% of pixels are within ± 0.05 FAPAR requirements (Figure 7) while only 63% and 65% of pixels meet this requirement when compared with GIMMS3g and GLASS, respectively. The highest differences are found over latitudes higher than 50°N in winter time where GEOV2-AVHRR show higher FAPAR values than GIMMS3g and GLASS (red tones in Figure 7). GIMMS3g product is not available for very high northern latitudes ($>60^{\circ}\text{N}$) in winter time (areas in grey in Figure 7). GIMMS3g FAPAR is also missing for bare soil areas and when available it is systematically higher than GEOV2-AVHRR for the areas with low mean FAPAR values (blue tones in Figure 7). The scatter plots show very strong agreement for GEOV2-AVHRR as compared to both GEOV2-CGLS and GLASS for all the range of FAPAR values (Figure 10) and biomes (Figure 13). Conversely the GIMMS3g FAPAR shows a positive bias for FAPAR<0.2 (Figure 10b) across biomes (Figure 13). This problem seems to be associated to the training dataset used to calibrate the GIMMS3g algorithm, in particular the MODIS products used for learning neural networks (Zhu et al. 2013). Note that a similar offset for the low FAPAR values was observed in MODIS product in previous validation studies (Martínez et al. 2013).

For FCOVER, a good agreement between GEOV2-AVHRR and GEOV2-CGLS is observed at the global scale (85% of pixels within 0.05 FCOVER difference, Figure 8) for all the range of values (Figure 11) and biomes (Figure 14) although GEOV2-AVHRR shows slightly lower maximum values than GEOV2-CGLS over deciduous (Figure 2) and needleleaf forest (Figure 3) for northern latitudes in summer time (Figure 8). The comparison between GEOV2-AVHRR and GLASS show that 57% of land pixels exhibit mean differences within ± 0.05 FCOVER although for northern high latitudes GLASS is systematically higher than GEOV2-AVHRR (Figure 8). The extremely low and high FCOVER values agree well but GLASS shows higher intermediate FCOVER values (Figure 11). The higher differences between GEOV2-AVHRR and GLASS FCOVER are observed over for deciduous and needleleaf forests (Figure 14) where GLASS systematically shows higher GLASS values (blue tones in Figure 8 for northern high latitudes). GLASS showed unexpected multimodal FCOVER distributions for needleleaf forests (Figure 14) and unexpected high FCOVER values in wintertime (Figure 2, Figure 3) which are inconsistently higher than FAPAR values (Figure 22).

In general, the agreement between GEOV2-AVHRR and other products is deteriorated when the number n of available observations in the composition period is lower than approximately five. These situations mostly correspond to land pixels close to tropical latitudes with permanent cloud coverage and high latitudes with snow coverage in winter time (Figure 15a). However, the distribution of n values (dashed line in Figure 15a) shows that it is between 5 and 20 in most situations. The difference between GEOV2-AVHRR and GEOV2-CGLS are closely linked to the uncertainty associated to the GEOV2-AVHRR product and computed as the RMSE between the final product values and the daily estimates in the compositing window (Figure 15b): higher LAI differences with higher RMSE values. Note that the distribution of RMSE values (dashed line in Figure 15b) shows that most values are lower than 0.1 LAI. Similar behavior is observed for FAPAR (Figure 16) and FCOVER (Figure 17), with however, a more limited range of variation of the difference GEOV2-AVHRR – GEOV2-CGLS and the associated RMSE values.

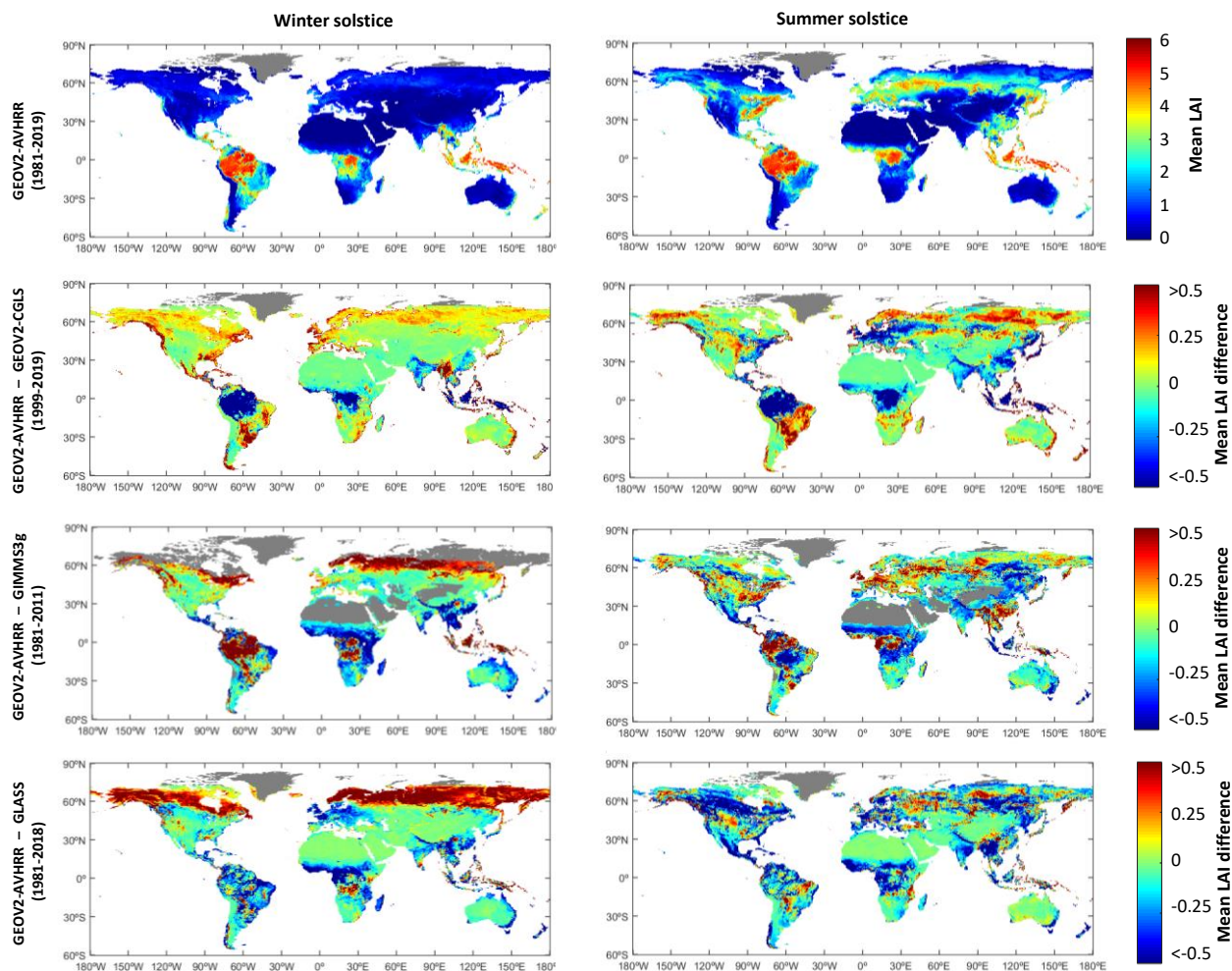


Figure 6: Mean GEOV2-AVHRR LAI values (top) and mean LAI differences between GEOV2-AVHRR and GEOV2-CGLS, GIMMS3g, and GLASS products for the common period for winter and summer solstice dates. Red (blue) tones in the maps of differences indicate positive (negative) differences, i.e. higher (lower) GEOV2-AVHRR values. The areas in grey correspond to pixels with no data.

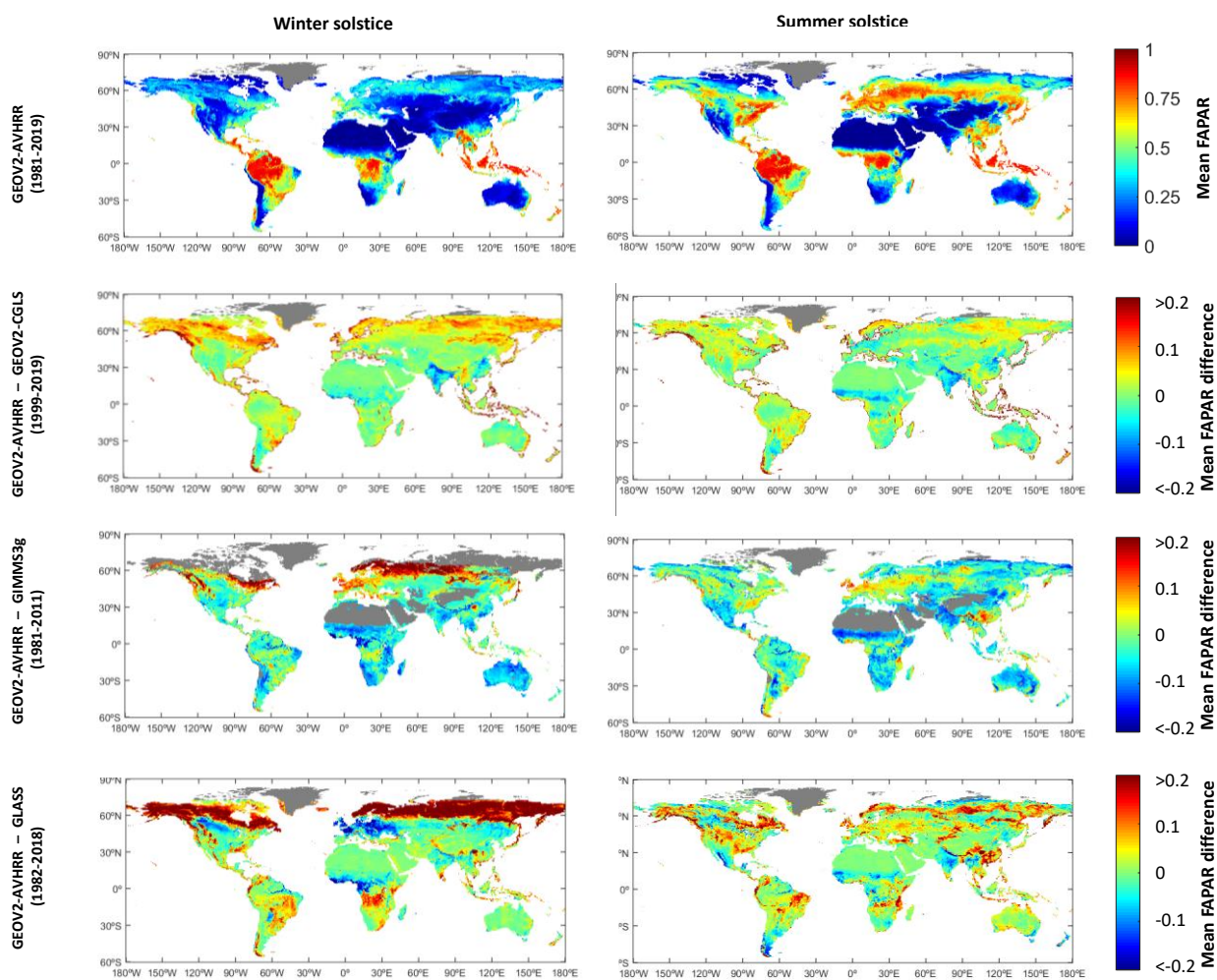


Figure 7: Idem Figure 6 but for FAPAR.

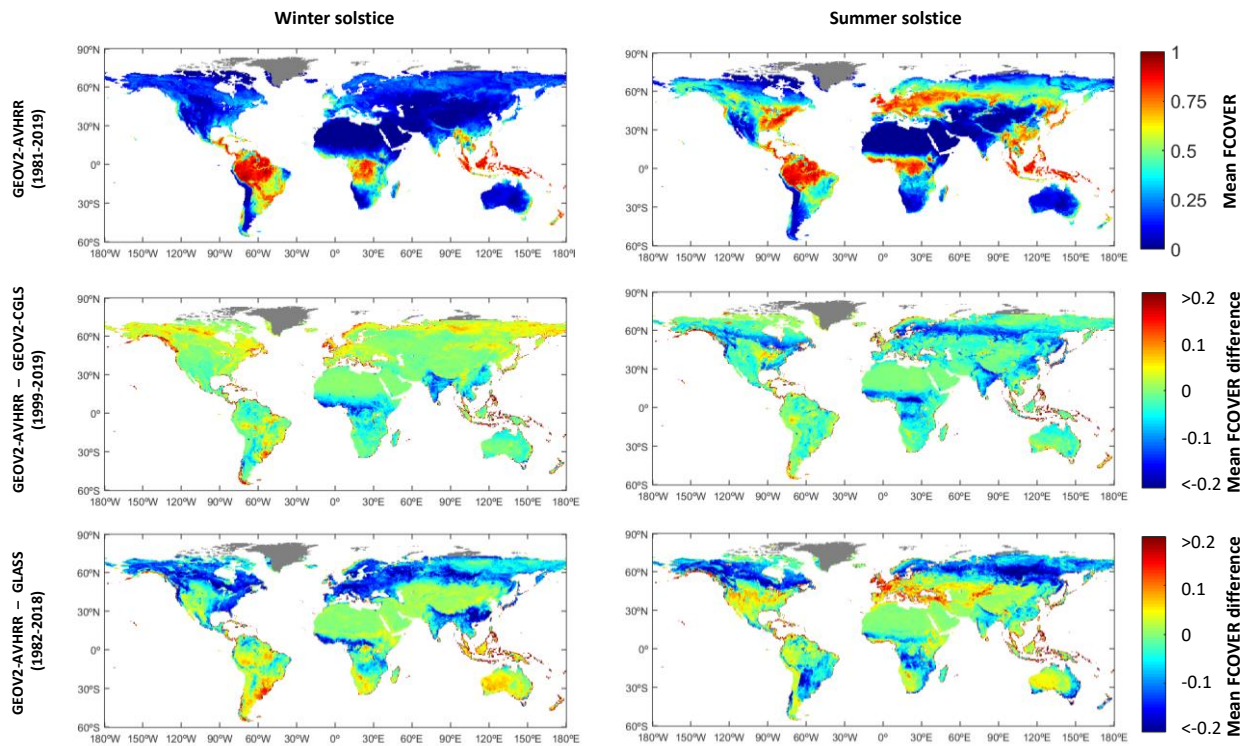


Figure 8: Idem Figure 6 but for FCOVER.

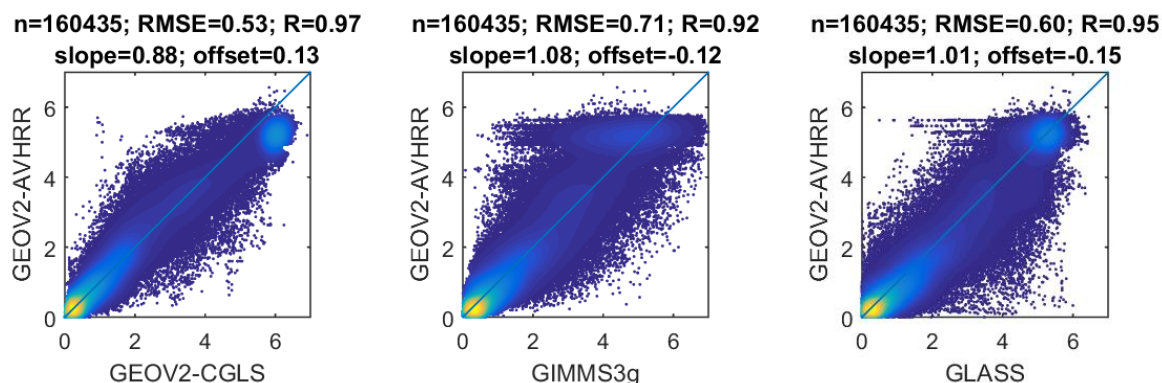


Figure 9: Comparison between GEOV2-AVHRR and (a) GEOV2-CGLS, (b) GIMMS3g, (c) GLASS LAI products over the BELMANIP2 sites for the 1999-2011 period.

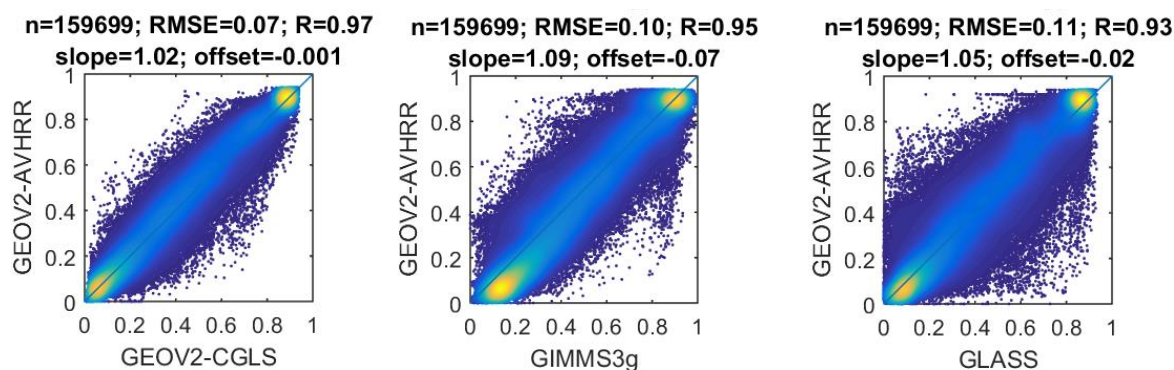


Figure 10: Comparison between GEOV2-AVHRR and (a) GEOV2-CGLS, (b) GIMMS3g, (c) GLASS FAPAR products over the BELMANIP2 sites for the 1999-2011 period.

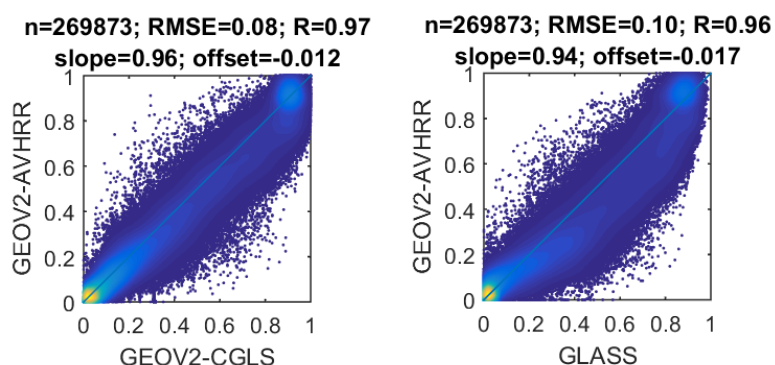


Figure 11: Comparison between GEOV2-AVHRR and (a) GEOV2-CGLS, (b) GLASS FCOVER products over the BELMANIP2 sites for the 2000-2016 period.

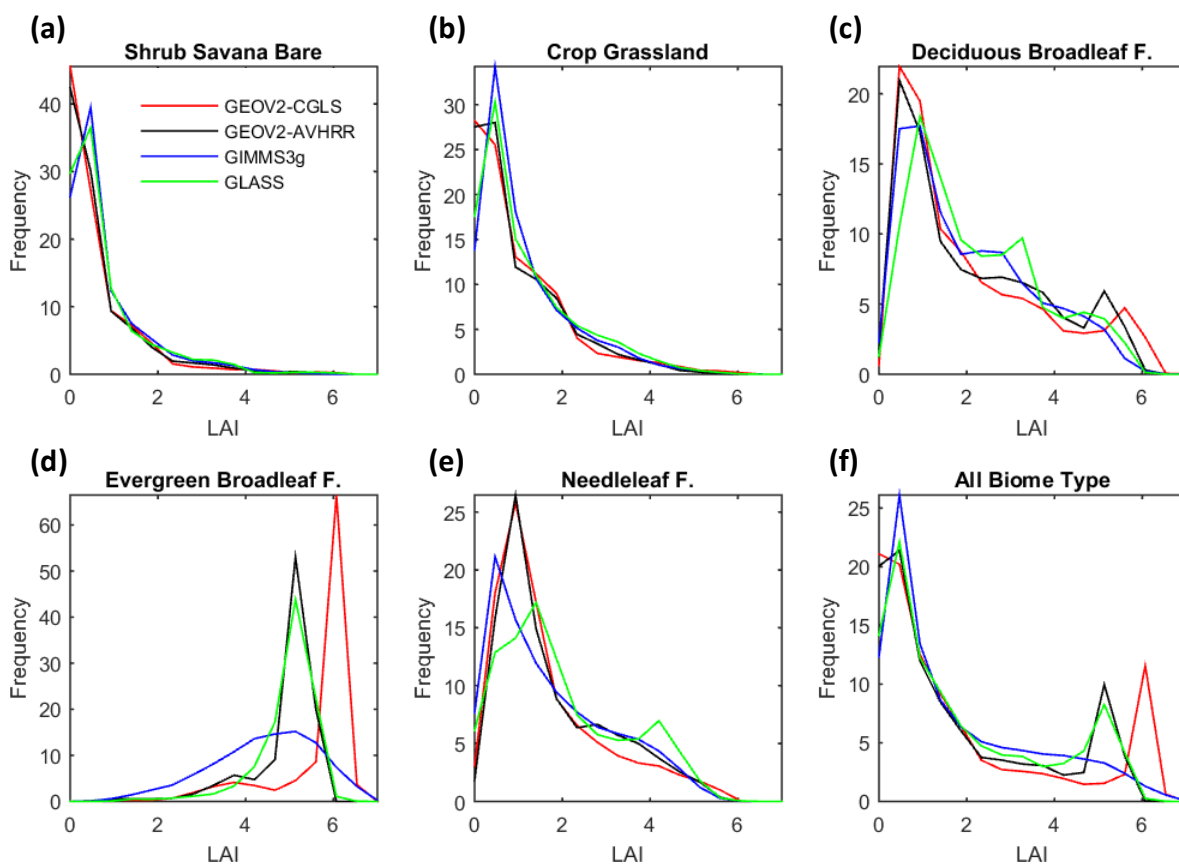


Figure 12: Distribution of GEOV2-AVHRR, GEOV2-CGLS, GIMMS3g and GLASS LAI products per CCI-LC biome type as sampled by the 445 BELMANIP2 sites over the 1999-2011 period.

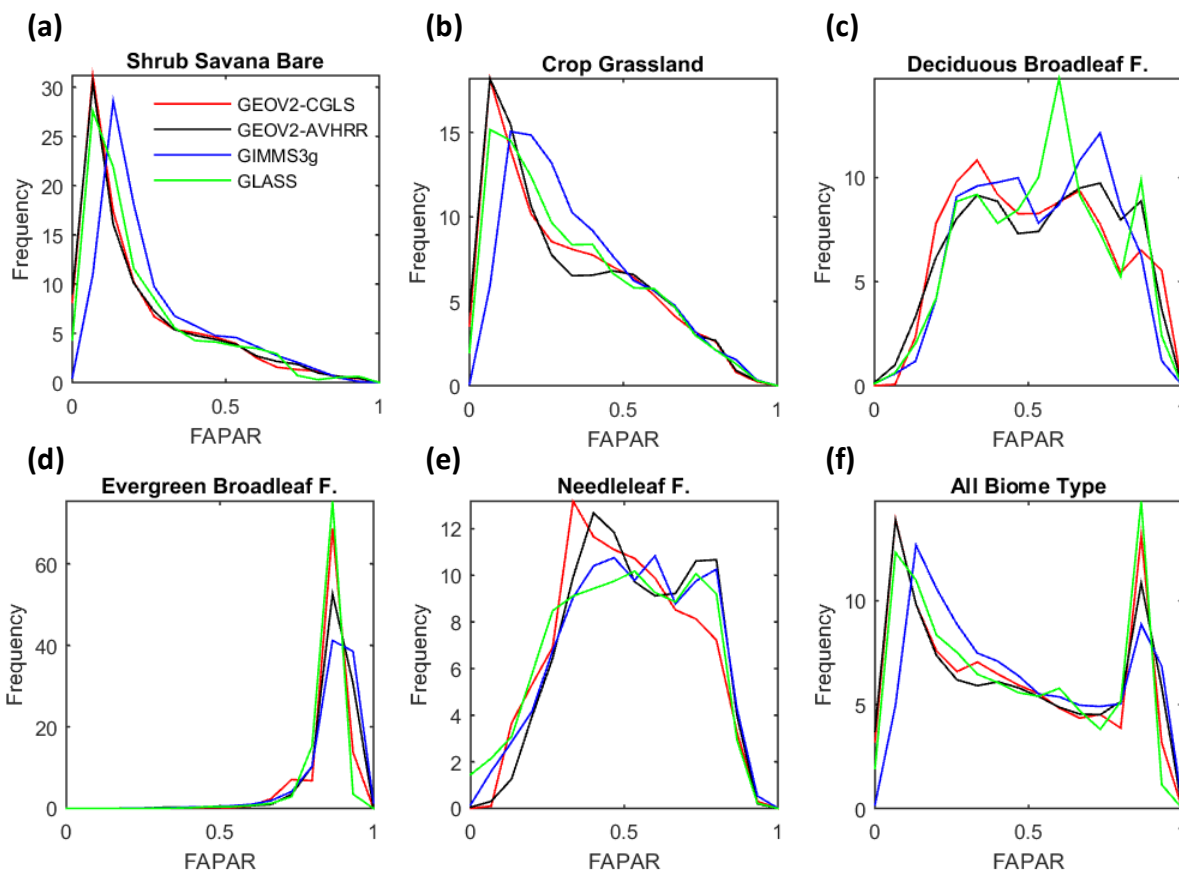


Figure 13: Distribution of GEOV2-AVHRR, GEOV2-CGLS, GIMMS3g and GLASS FAPAR products per CCI-LC biome type as sampled by the 445 BELMANIP2 sites over the 1999-2011 period.

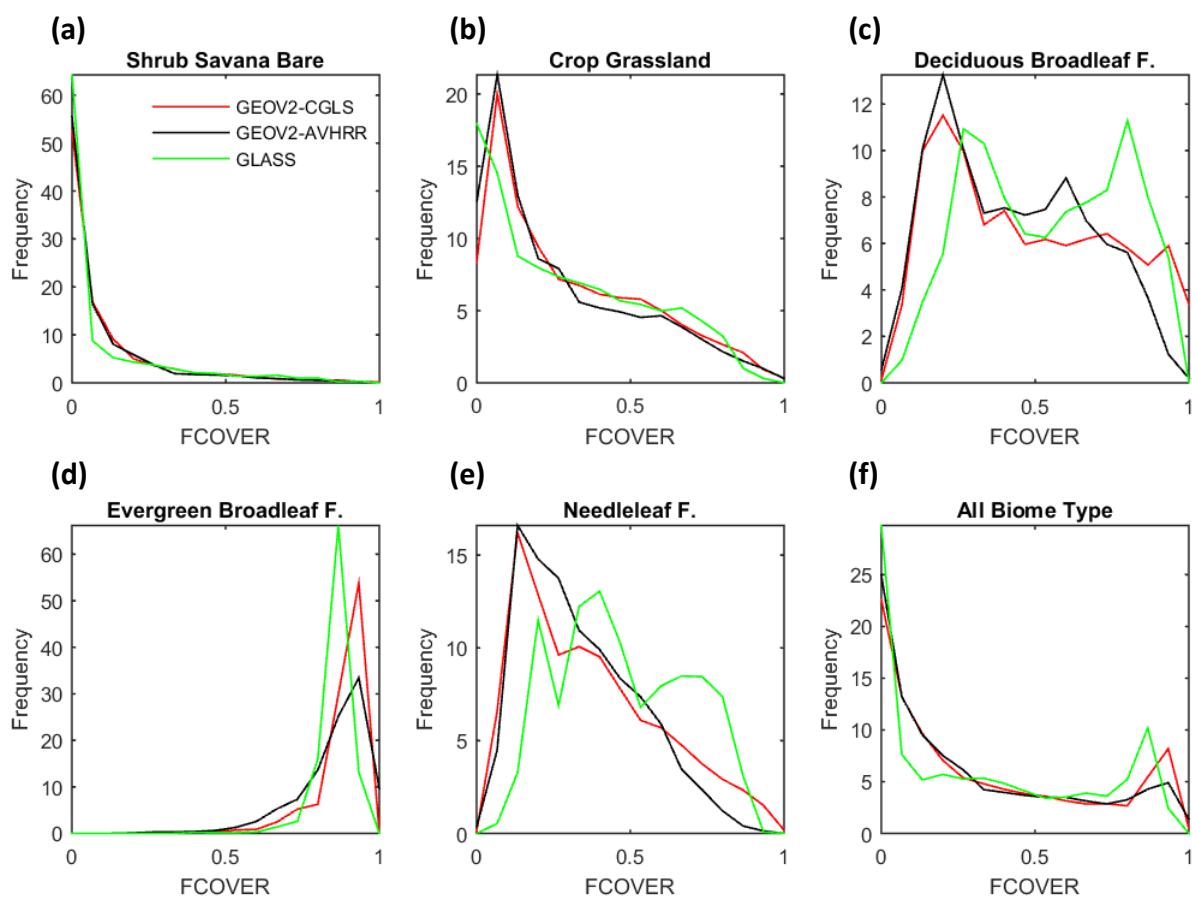


Figure 14: Distribution of GEOV2-AVHRR, GEOV2-CGLS and GLASS FCOVER products per CCI-LC biome type as sampled by the 445 BELMANIP2 sites over the 1999-2018 period.

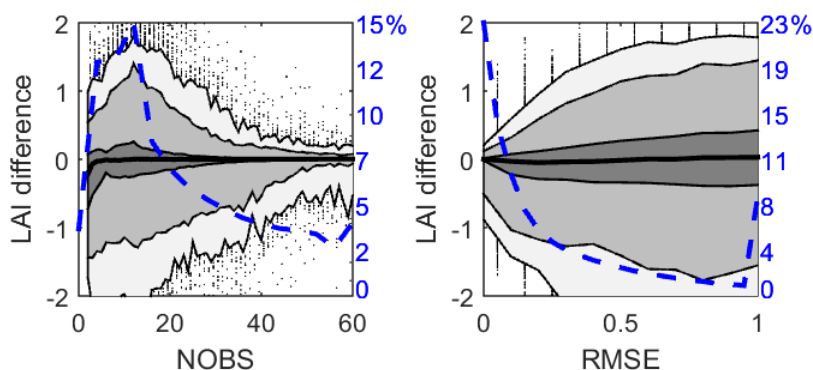


Figure 15: Evaluation of the differences between GEOV2-AVHRR and GEOV2-CGLS LAI products over the BELMANIP2.1 sites for the years 1999-2019 as a function of (a) the number of valid AVHRR observations in the compositing period (NOBS) and (b) the GEOV2-AVHRR product uncertainty (i.e., RMSE between the GEOV2-AVHRR product and the daily AVHRR observations in the compositing period). The gray levels correspond to 75% (dark gray), 90% (medium gray) and 95% (light gray) of the population, and the dots to 5% percentile of the residual outliers. The bold back solid line corresponds to the median value of the differences. The blue dashed line shows the distribution of values of the variable in the abscissa which frequencies are indicated in the vertical axis on the right.

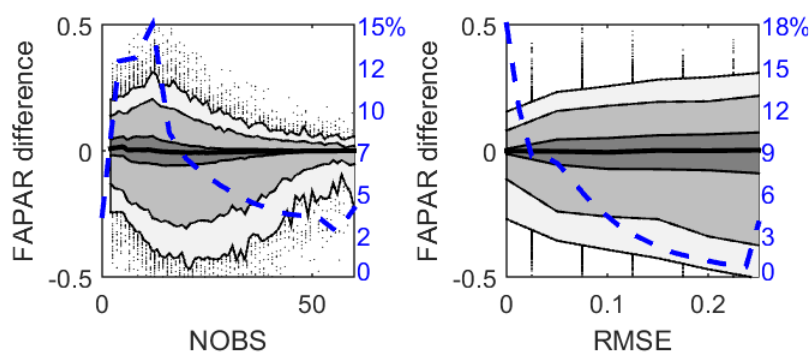


Figure 16: Idem Figure 15 but for FAPAR

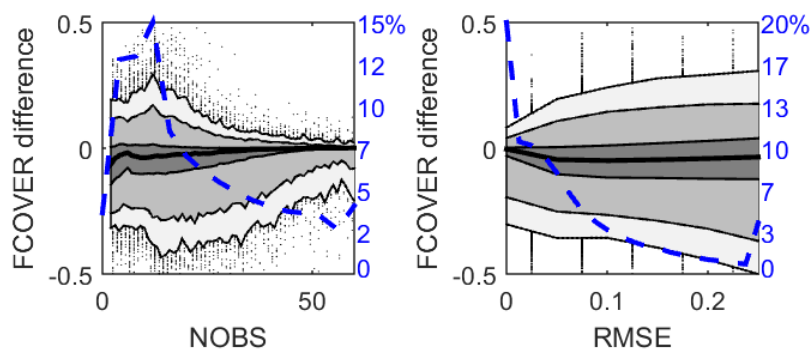


Figure 17: Idem Figure 15 but for FCOVER

2.3 SPATIO-TEMPORAL CONTINUITY

The fraction of missing data is 5% for GEOV2-AVHRR (and GEOV2-CGLS, not shown), 28% for GIMMS3g and less than 1% for GLASS (not shown) during the 1981-2011 period (Figure 18, Figure 19). GIMMS is not processed for pixels flagged as bare soil according to the MODIS land cover. GEOV2-AVHRR is only missing in Greenland and latitudes $>70^{\circ}\text{N}$ when the climatology is not available. The map of the mean fraction of filled GEOV2-AVHRR data shows that gap filling (less than 6 observations in the 60-days semi-window) mainly occurs in tropical latitudes around the equator and northern high latitudes (Figure 18a). The climatological values are used to fill large gaps in 5% to 75% of the cases depending on the biome type as displayed in Figure 19. Evergreen broadleaf forests, which are mostly located in areas with continuous cloud cover around the equator, have the highest fraction of gap filled data. The highest discontinuities in GIMMS3g product are observed (Figure 19) for Shrub/Savana/Bare biome type with a fraction of missing data of 60% since pixels flagged as bare areas according to the MODIS landcover product are not processed (grey areas in Figure 18b).

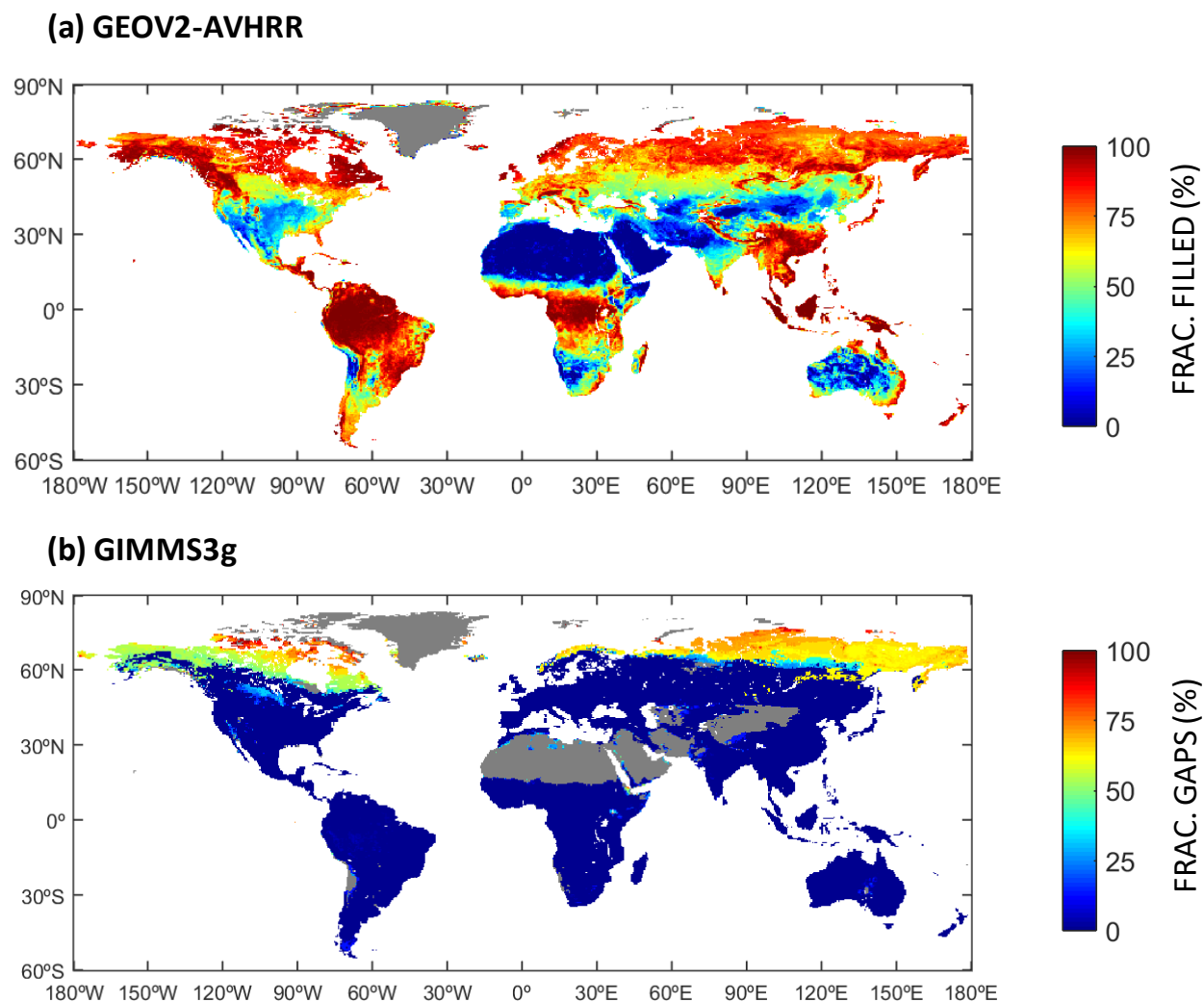


Figure 18: (a) Map of the fraction of filled data for which the climatology or the linear interpolation is used for processing GEOV2-AVHRR products. (b) Map of the fraction of gaps for GIMMS3g products. The areas in grey correspond to unprocessed pixels (missing data). Evaluation for the 1981-2011 period.

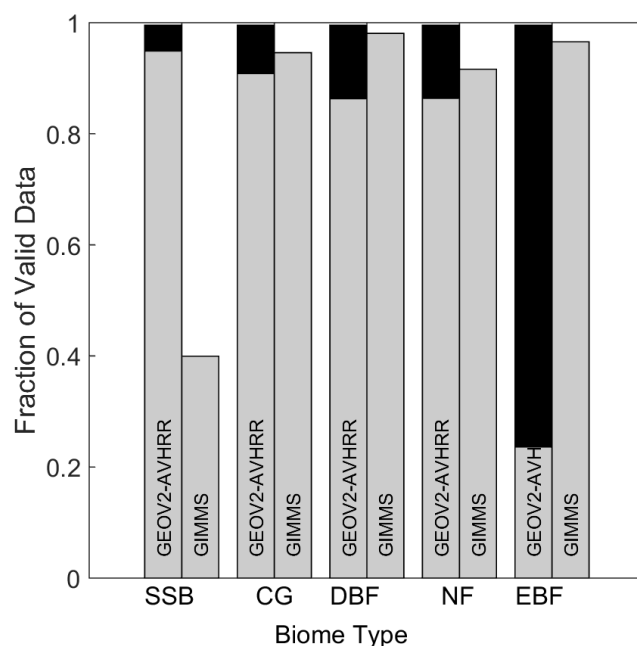


Figure 19: Average fraction of valid GEOV2-AVHRR and GIMMS3g products per biome. The biome classes are derived from the CCI landcover map (http://maps.elie.ucl.ac.be/CCI/viewer/download/ESACCI-LC-Ph2-PUGv2_2.0.pdf): Shrubs/Savana/Bare soil (SSB), Crops and Grassland (CG), Deciduous Broadleaf Forests (DBF), Needleleaf Forest (NF), and Evergreen Broadleaf Forest (EBF). For GEOV2/AVHRR, high quality products (grey) and products where the climatology was used to fill gaps (less than 12 valid daily estimates exist in the compositing period) (black) are distinguished. Evaluation over the BELMANIP2 sites for the 1981-2011 period.

2.4 TEMPORAL SMOOTHNESS

LAI variable results from incremental bio-physical processes. It is therefore expected to show relatively smooth temporal variations except in extreme situations such as flooding, fire or changes in the land-use. High variability in the temporal profiles would indicate a lack of reliability of the derived products. The smoothness of the LAI temporal series was evaluated based on the absolute value of the difference, δLAI , between $LAI(t)$ product value at date t and the mean value between the two closest bracketing dates in a maximum Δt period of 60 days: $\delta LAI = |1/2(LAI(t + \Delta t) + LAI(t - \Delta t)) - LAI(t)|$ (Verger et al. 2011). The smoother the temporal evolution, the smaller the δ difference should be. The histogram of δ over the whole dataset of BELMANIP2 sites in the 2000-2011 period (Figure 20) shows that both GEOV2-AVHRR and GEOV2-CGLS products are very smooth with differences lower than 0.1 LAI for most of cases. GEOV2-AVHRR and GEOV2-CGLS show intermediate distributions as compared to GIMMS and GLASS (Figure 20). The GLASS product shows the smoothest temporal evolution at expenses of miss reproducing rapid variations in the temporal evolution of LAI as illustrated in the double-cycle cropland site #337 in Figure 4. On

the opposite, GIMMS3g shows the highest frequencies for higher δ values indicating a shakier temporal evolution as illustrated in Figure 1.

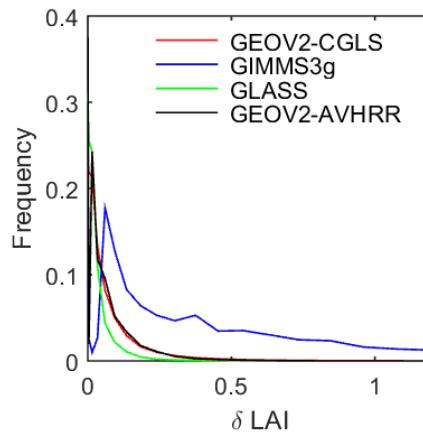


Figure 20: Histogram of the δ LAI absolute difference representing temporal smoothness for GEOV2-AVHRR, GEOV2-CGLS, GIMMS3g and GLASS LAI products. Evaluation over the BELMANIP2 sites for the 1999-2011 period.

2.5 CONSISTENCY BETWEEN LAI, FAPAR AND FCOVER PRODUCTS

In terms of internal consistency, GEOV2-AVHRR and GEOV2-CGLS show a LAI-FAPAR exponential dependency as expected (Myneni and Williams 1994) (Figure 21). Indeed, while this product consistency is ensured by the fused MODIS and CYCLOPES product used to train the neural networks, it is still maintained when applying the compositing algorithm. The LAI-FAPAR relationship for GEOV2-AVHRR and GEOV2-CGLS show high consistency for all the range of values with non-artifacts introduced by the use of two different processing schemes: one for EBFs and one for non EBFs classes. For GIMMS3g and GLASS products, higher scattering is observed and different patterns in the LAI-FAPAR relationship that may be introduced by the biome dependency of the MODIS products used for calibrating the retrieval algorithm (Myneni et al. 2002).

GEOV2-AVHRR and GEOV2-CGLS show also very consistent FAPAR-FCOVER relationships with $FAPAR > FCOVER$ (Figure 22). Indeed, when normalized by its maximum value, FAPAR can be approximated by the FIPAR (Fraction of Intercepted Photosynthetically Active Radiation), which is the complementary of the gap fraction at the sun angle corresponding to 10:00 am solar time for a given pixel, and thus, leading to a higher value than FCOVER defined as the complementary to the gap fraction in the nadir direction. GLASS products show more inconsistencies: higher scattering, unexpected lower FAPAR than FCOVER for intermediate values and a positive bias of FAPAR for FCOVER values close to zero (Figure 22). These inconsistencies between GLASS variables are due, in part, to the different retrieval algorithms used for LAI/FAPAR (Xiao et al. 2015) and FCOVER (Jia et al. 2019).

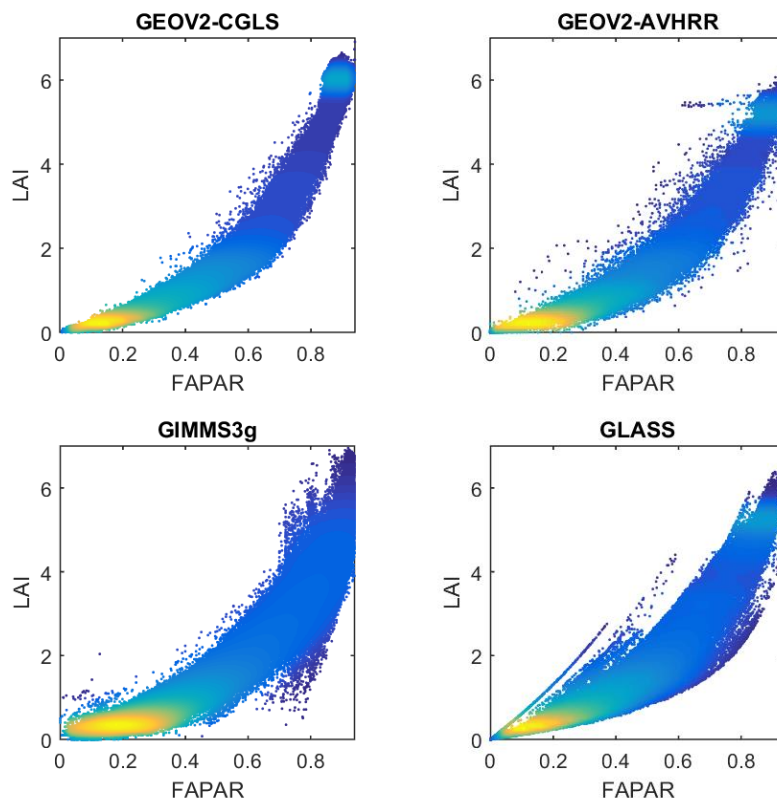


Figure 21: Relationship between LAI and FAPAR for GEOV2-CGLS, GEOV2-AVHRR, GIMMS3g and GLASS products as evaluated over the 445 BELMANIP2.1 sites during the 1999-2011 period. The color indicates the density of points from yellow (highest) to blue (lowest density).

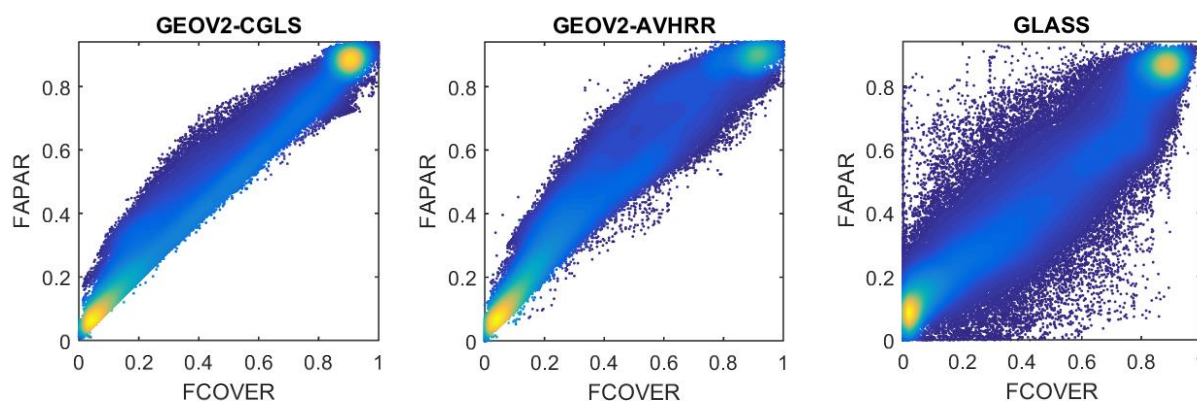


Figure 22: Relationship between FAPAR and FCOVER for GEOV2-CGLS, GEOV2-AVHRR and GLASS products as evaluated over the 445 BELMANIP2.1 sites during the 2000-2011 period. The color indicates the density of points from yellow (highest) to blue (lowest density).

2.6 COMPARISON WITH GROUND DATA

More quantitative assessment was achieved using the available ground-based measurements acquired over 3 km x 3 km DIRECT 2.0 sites in the 1999-2017 period (<http://calvalportal.ceos.org/web/olive/site-description>). Each product was interpolated at the date of the ground measurements if two valid dekadal data exist within a maximum period of ± 30 days. For comparison purposes, the different satellite products (GEOV2-AVHRR, GEOV2-CGLS, GIMMS3g and GLASS) were also validated over the common samples where all products were available. The comparison of GEOV2-AVHRR with the ground-based observations of LAI, FAPAR and FCOVER variables shows respectively an overall RMSE of 0.81, 0.10 and 0.13 (Figure 23, Table 1). Similar performances are found for the other satellite products when evaluated over the same ground dataset (Table 1). However, this validation is limited by the low number of available ground-based measurements that were mostly achieved in non-problematic conditions close to the maximum peak of vegetation. Further confrontation with ground based data is required, particularly over sites located at equatorial regions or very high latitude where higher noise and occurrence of missing data is expected in the satellite surface reflectance data. The validation is also affected by the uncertainty associated to reference maps which is expected to be around 1 LAI units for forest (Fernandes et al. 2003) or around 0.5 LAI for croplands (Martínez et al. 2009) and up to 0.1 for FAPAR (Gobron et al. 2008) and FCOVER (Verger et al. 2009).

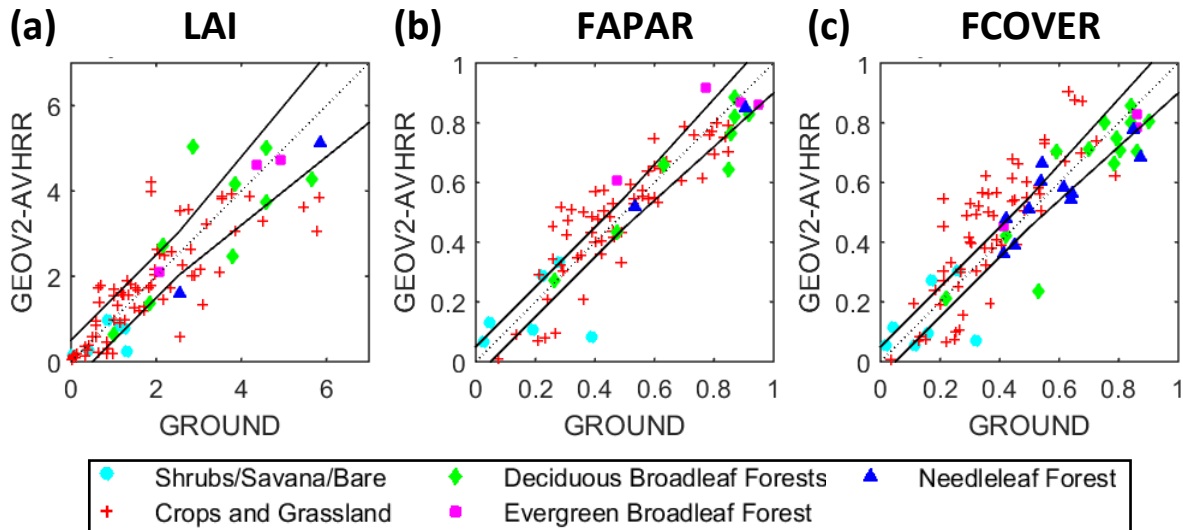


Figure 23: Comparison of GEOV2-AVHRR with ground measurements for (a) LAI, (b) FAPAR and (c) FCOVER in the 1999-2017 period. The different symbols correspond to the five biome classes as derived from the CCI landcover map (http://maps.elie.ucl.ac.be/CCI/viewer/download/ESACCI-LC-Ph2-PUGv2_2.0.pdf). The dotted line corresponds to the 1:1 line. The solid lines represent the GCOS accuracy criteria: max(20%, 0.5) for LAI, max(10%, 0.05) for FAPAR (and FCOVER) (GCOS 2011). The statistics of the comparison are provided in Table 1.

Table 1: Statistics of the comparison of GEOV2-AVHRR, GEOV2-CGLS, GIMMS3g and GLASS with ground measurements for LAI, FAPAR and FCOVER variables over the DIRECT2 sites for the common samples in the 1999-2017 period: number of sites, number of samples (sites x dates), percentage of samples which meet GCOS requirements in terms of accuracy (max(20%, 0.5) for LAI, max(10%, 0.05) for FAPAR (and FCOVER) (GCOS 2011)), root mean square error (RMSE), correlation coefficient (R), slope and offset of the least squares linear regression. (*) Statistics of the validation of GEOV2-AVHRR over all available samples in the 1999-2017 period.

		Num. samples	%OK GCOS	RMSE	R	slope	offset
LAI	GEOV2-AVHRR*	95	63	0.81	0.85	0.79	0.26
	GEOV2-AVHRR	49	69	0.74	0.89	0.82	0.06
	GEOV2-CGLS	49	67	0.91	0.86	0.84	0.05
	GIMMS3g	49	59	0.84	0.86	0.62	0.29
	GLASS	49	76	0.84	0.86	0.98	0.09
FAPAR	GEOV2-AVHRR*	79	48	0.10	0.91	0.87	0.07
	GEOV2-AVHRR	31	58	0.09	0.94	0.93	0.03
	GEOV2-CGLS	31	61	0.08	0.96	0.94	0.05
	GIMMS3g	31	52	0.09	0.93	0.84	0.08
	GLASS	31	61	0.07	0.96	0.95	0.01
FCOVER	GEOV2-AVHRR	97	35	0.13	0.85	0.90	0.08
	GEOV2-CGLS	97	27	0.15	0.91	1.03	0.09
	GLASS	97	31	0.13	0.88	1.01	0.05

3 CONCLUSION

The GEOV2-AVHRR LAI, FAPAR and FCOVER products capitalize on the efforts undertaken to pre-process the AVHRR temporal series, resulting in the LTDR data (Vermote et al. 2009), and the recent development of improved processing of biophysical products resulting in the GEOV2-CGLS dataset (Verger et al. 2014). The GEOV2-AVHRR algorithm was designed to provide smooth and continuous time series and special emphasis was put on achieving consistency with GEOV2-CGLS products. This document presents a Quality Assessment of GEOV2-AVHRR LAI, FAPAR and FCOVER products for the 1981-2019 period. The comparison of GEOV2-AVHRR with GEOV2-CGLS indicates a very good agreement between the two datasets with a similar level of accuracy as evaluated through the comparison with ground-based measurements. An improvement in terms of temporal consistency and continuity is achieved in GEOV2-AVHRR products as compared to GLASS and GIMMS3g AVHRR products.

4 REFERENCES

- Fernandes, R., Burton, C., Leblanc, S., & Latifovic, R. (2003). Landsat-5 TM and Landsat-7 ETM+ based accuracy assessment of leaf area index products for Canada derived from SPOT-4 VEGETATION data. *Canadian Journal of Remote Sensing*, 20, 241-258
- GCOS (2011). -Global Climate Observing System - Systematic Observation Requirements for Satellite-Based Products for Climate - 2011 Update, Supplemental Details to the Satellite Based Component of the Implementation Plan for the Global Observing System for Climate in Support of the UNFCCC (2010 Update), . In (p. 138). Geneva, Switzerland: World Meteorological Organization
- Gobron, N., Pinty, B., Ausedat, O., Taberner, M., Faber, O., Mélin, F., Lavergne, T., Robustelli, M., & Snoeij, P. (2008). Uncertainty estimates for the FAPAR operational products derived from MERIS — Impact of top-of-atmosphere radiance uncertainties and validation with field data. *Remote Sensing of Environment*, 112, 1871-1883
- Jia, K., Yang, L., Liang, S., Xiao, Z., Zhao, X., Yao, Y., Zhang, X., Jiang, B., & Liu, D. (2019). Long-Term Global Land Surface Satellite (GLASS) Fractional Vegetation Cover Product Derived From MODIS and AVHRR Data. *IEEE Journal of Selected Topics in Applied Earth Observations and Remote Sensing*, 12, 508-518
- Liang, S., Zhao, X., Liu, S., Yuan, W., Cheng, X., Xiao, Z., Zhang, X., Liu, Q., Cheng, J., Tang, H., Qu, Y., Bo, Y., Qu, Y., Ren, H., Yu, K., & Townshend, J. (2013). A long-term Global Land Surface Satellite (GLASS) data-set for environmental studies. *International Journal of Digital Earth*, 6, 5-33
- Martínez, B., Camacho, F., Verger, A., García-Haro, F.J., & Gilabert, M.A. (2013). Intercomparison and quality assessment of MERIS, MODIS and SEVIRI FAPAR products over the Iberian Peninsula. *International Journal of Applied Earth Observation and Geoinformation*, 21, 463-476
- Martínez, B., García-Haro, F.J., & Camacho-de Coca, F. (2009). Derivation of high-resolution leaf area index maps in support of validation activities: Application to the cropland Barrax site. *Agricultural and Forest Meteorology*, 149, 130-145
- Myneni, R.B., Hoffman, S., Knyazikhin, Y., Privette, J.L., Glassy, J., Tian, Y., Wang, Y., Song, X., Zhang, Y., Smith, G.R., Lotsch, A., Friedl, M., Morisette, J.T., Votava, P., Nemani, R.R., & Running, S.W. (2002). Global products of vegetation leaf area and absorbed PAR from year one of MODIS data. *Remote Sensing of Environment*, 83, 214-231
- Myneni, R.B., & Williams, D.L. (1994). On the relationship between FAPAR and NDVI. *Remote sensing of the environment*, 49, 200-211
- Verger, A., Baret, F., & Weiss, M. (2011). A multisensor fusion approach to improve LAI time series. *Remote Sensing of Environment*, 115, 2460-2470
- Verger, A., Baret, F., & Weiss, M. (2014). Near real time vegetation monitoring at global scale. *IEEE Journal of Selected Topics in Applied Earth Observations and Remote Sensing*, 7, 3473-3481
- Verger, A., Baret, F., & Weiss, M. (2016). GIO Global Land Component - Algorithm Theoretical Basis Document - Leaf Area Index (LAI), Fraction of Absorbed Photosynthetically Active Radiation (FAPAR) and Fraction of green Vegetation Cover (FCover) Version 2.0 (GEOV2), Issue I1.31. In (p. 78). Barcelona: CREAM
- Verger, A., Baret, F., Weiss, M., Filella, I., & Peñuelas, J. (2015). GEOCLIM: A global climatology of LAI, FAPAR, and FCOVER from VEGETATION observations for 1999–2010. *Remote Sensing of Environment*, 166, 126-137
- Verger, A., Martínez, B., Camacho-de Coca, F., & García-Haro, F.J. (2009). Accuracy assessment of fraction of vegetation cover and leaf area index estimates from pragmatic methods in a cropland area. *International Journal of Remote Sensing*, 30, 2685 - 2704
- Vermote, E., Justice, C., Csiszar, I., Eidenshink, J., Myneni, R., Baret, F., Masuoka, E., & Wolfe, R. (2009). A Terrestrial Surface Climate Data Record for Global Change Studies. In, *Fall Meeting, San-*

Francisco (USA): Eos Transactions, Suppl., v. 90, no. 52: Washington, D.C., American Geophysical Union, abstract number IN42A-08. (Also available online at <http://www.agu.org/meetings/fm09/waisfm09adv.html>.)

Xiao, Z., Liang, S., Sun, R., Wang, J., & Jiang, B. (2015). Estimating the fraction of absorbed photosynthetically active radiation from the MODIS data based GLASS leaf area index product. *Remote Sensing of Environment*, 171, 105-117

Zhu, Z., Bi, J., Pan, Y., Ganguly, S., Anav, A., Xu, L., Samanta, A., Piao, S., Nemani, R., & Myneni, R. (2013). Global Data Sets of Vegetation Leaf Area Index (LAI)3g and Fraction of Photosynthetically Active Radiation (FPAR)3g Derived from Global Inventory Modeling and Mapping Studies (GIMMS) Normalized Difference Vegetation Index (NDVI3g) for the Period 1981 to 2011. *Remote Sensing*, 5, 927-948